the DNA from isolated chromosomes has high molecular weight. Thus, sorter-purified DNA is suitable for gene mapping and for production of recombinant DNA libraries. However, additional development may be required if considerably larger amounts of DNA are required for such applications as analysis of large restriction fragments by pulsed-field gel electrophoresis (*34*) and cloning in yeast (*35*). Increases in the sort rate may come from several areas: (i) use of velocity sedimentation to enrich the chromosome of interest before sorting (*36*), (ii) production of hybrids or other cell lines in which the frequency of the chromosome of interest is high (for example, human-muntjac hybrids to which the muntjac contributes only three chromosome types), (iii) further increases in the droplet production rate in the high-speed sorter, and (iv) increased distinctness in chromosome staining so that high-purity sorting can be accomplished while objects are processed at rates of over 20,000 per second. Taken together, these developments eventually may lead to another order of magnitude increase in the rate at which chromosomes can be purified by sorting.

REFERENCES AND NOTES

1. V. McKusick, *Cold Spring Harbor Symp. Quant. Biol.* **51**, 15 (1986).
2. T. Caskey, *ibid.*, p. 1115.
3. J. W. Gray *et al.*, *Proc. Natl. Acad. Sci. U.S.A.* **72**, 1231 (1975).
4. J. W. Gray and R. G. Langlois, *Annu. Rev. Biophys. Biophys. Chem.* **15**, 195 (1986).
5. L. L. Deaven *et al.*, *Cold Spring Harbor Symp. Quant. Biol.* **51**, 159 (1986).
6. S. A. Latt *et al.*, in *Flow Cytogenetics*, J. Gray, Ed. (Academic Press, New York, in press).
7. R. Lebo, *Cytometry* **3**, 145 (1982).
8. D. C. Peters *et al.*, *ibid.* **6**, 290 (1985).
9. G. J. van den Engh, B. J. Trask, J. W. Gray, R. G. Langlois, L.-C. Yu, *ibid.*, p. 92.
10. R. Sillar and B. Young, *J. Histochem. Cytochem.* **29**, 74 (1981).
11. J. W. Gray, R. G. Langlois, A. V. Carrano, K. Burkhart-Schultz, M. A. Van Dilla, *Chromosoma (Berlin)* **73**, 9 (1979).
12. Derived from a computer model of a flow karyotype in which the peaks are approximated by bivariate normal distributions (J. W. Gray, unpublished).
13. D. Pinkel, T. Straume, J. W. Gray, *Proc. Natl. Acad. Sci. U.S.A.* **83**, 2934 (1986).
14. M. A. Van Dilla *et al.*, *Biotechnology* **4**, 537 (1986).
15. J. Perlman and J. C. Fuscoe, *Cytogenet. Cell Genet.* **43**, 87 (1986).
16. E. Hildebrand, personal communication; J. Fuscoe, personal communication.
17. R. Lebo *et al.*, *Cold Spring Harbor Symp. Quant. Biol.* **51**, 169 (1986).
18. L. Deaven *et al.*, personal communication.
19. R. Durand and P. L. Olive, *J. Histochem. Cytochem.* **30**, 111 (1982).
20. J. Visser, S. Bol, G. van den Engh, *Exp. Hematol.* **9**, 644 (1981).
21. B. Libbus, S. Perrault, L. Johnson, D. Pinkel, *Mutat. Res.*, in press.
22. N. Kanda *et al.*, *Proc. Natl. Acad. Sci. U.S.A.* **80**, 4069 (1983).
23. P. Scambler *et al.*, *Nucleic Acids Res.* **14**, 1951 (1986).
24. M. Lalande *et al.*, *Cancer Genet. Cytogenet.* **13**, 283 (1984).
25. T. A. Donlon *et al.*, *Proc. Natl. Acad. Sci. U.S.A.* **83**, 4408 (1986).
26. M. Krumlauf, M. Jeanpierre, B. D. Young, *ibid.* **79**, 2871 (1982).
27. K. A. Davies *et al.*, *Nature (London)* **293**, 374 (1981).
28. C. R. Muller *et al.*, *Hum. Genet.* **64**, 110 (1983).
29. C. M. Disteche *et al.*, *Cytometry* **2**, 282 (1982).
30. B. Baron *et al.*, *Somatic Cell Mol. Genet.* **12**, 289 (1986).
31. J. K. Griffith *et al.*, *Nucleic Acids Res.* **12**, 4019 (1984).
32. J. C. Fuscoe, L. M. Clark, M. A. Van Dilla, *Cytogenet. Cell Genet.* **43**, 79 (1986).
33. The statistical probability of any particular sequence being in a library of five chromosome equivalents is 0.99. Since fragments larger than 9.1 kb cannot be cloned in Charon 21A, 35% of the DNA mass is unclonable. Thus, the probability of a particular sequence being in either the Hind III or Eco RI library is $0.99 - (0.35)(0.35) \simeq 90\%$ (*32*).
34. D. C. Schwartz and C. R. Cantor, *Cell* **37**, 67 (1984).
35. D. T. Burke, G. F. Carle, M. V. Olson, *Science* **236**, 806 (1987).
36. J. G. Collard *et al.*, *Exp. Cell Res.* **138**, 217 (1980).
37. T. C. Gilliam *et al.*, *Nucleic Acids Res.* **15**, 1445 (1987).
38. L. M. Davis, N. J. Nowak, T. B. Shows, *Am. J. Hum. Genet. Suppl.* (1987), p. A212.
39. T. Keith *et al.*, *ibid.*, p. A508; V. Hyland, personal communication.
40. P. Van Tuinen, personal communication.
41. J. C. Fuscoe *et al.*, in preparation.

42. This work was performed under the auspices of the U.S. Department of Energy, Office of Health and Environmental Research by the Lawrence Livermore National Laboratory under contract number W-7405-ENG-48 with the support of USPHS grant HD17655. We thank L. Mitchell for expert help in the production of this manuscript. A probe complementary to centromeric sequences on chromosome 16 was provided by R. Moyzis, Los Alamos National Laboratory, and a probe complementary to centromeric sequences on chromosome 17 was provided by H. Willard, University of Toronto.

Magnetoencephalography and Epilepsy Research

D. F. ROSE, P. D. SMITH, S. SATO

Magnetoencephalography is the detection of the magnetic field distribution across the surface of the head, which is generated by a neuronal discharge within the brain. Magnetoencephalography is used in clinical epilepsy to localize the epileptogenic region prior to its surgical removal. A discussion of the instrumentation based on the superconducting quantum interference device that is used for detecting the magnetic field distribution, the analytical techniques, current research, and future directions of magnetoencephalography in epilepsy research is presented.

D. F. Rose, Medical Neurology Branch, National Institute of Neurological and Communicative Disorders and Stroke, National Institutes of Health, Bethesda, MD 20892. P. D. Smith, Biomedical Engineering and Instrumentation Branch, Division of Research Services, National Institutes of Health, Bethesda, MD 20892. S. Sato, EEG Laboratory, National Institute of Neurological and Communicative Disorders and Stroke, National Institutes of Health, Bethesda, MD 20892.

MAGNETOENCEPHALOGRAPHY (MEG) IS THE MEASUREment of the extracranial magnetic fields produced by electrical currents within the brain. These spontaneous magnetic fields are about one-billionth the strength of the earth's magnetic field and are measurable only with a superconducting quantum interference device (SQUID). The electrical currents arise from ion movements produced by changes in the electrical potential of cell membranes of neurons in the brain (Fig. 1). The changes in the membrane potential and ion movements usually begin at one end of the neuron called the dendrite, and compensatory ion movements occur throughout the neuronal cell body, creating a current dipole. We will refer to the current within the cell as the source current and the return current outside the cell as the volume current. The neurons of interest in MEG are the pyramidal cells, which are oriented perpendicular to the brain surface in a thin outer layer of the brain called the cortex, where many such neurons are aligned parallel to one another. The surface of the brain has many

infoldings producing "valleys" or sulci, and "hills" or gyri. The pyramidal cells may be broadly classified into two groups according to their orientation: (i) cells oriented perpendicular to the scalp surface, that is, aligned in a radial direction from the "center" of the head and (ii) cells oriented parallel to the surface of the scalp. These orientations correspond to radial and tangential current dipole sources, respectively (Fig. 1). Neurons that are oriented neither radially nor tangentially can be represented by components of the dipole in each of these directions.

The orientation of the current dipole is a critical factor affecting the measurement of magnetic fields outside the head. The magnetic field associated with a current dipole encircles the dipole and is oriented at right angles to the direction of the dipole (Fig. 2). When the axis of the SQUID gradiometer is oriented perpendicular to the subject's head, it measures only the component of the magnetic field perpendicular to the head surface. This magnetic field component, which has field lines perpendicular to the surface, is predominantly associated with the intracellular source currents of tangentially oriented dipoles. The reason for this can be understood in terms of a model that approximates the properties of the head. In a sphere of homogeneous electrical conductivity, a radially oriented dipole does not contribute to the magnetic field. Volume currents associated with a dipole in the sphere do not contribute to the perpendicular magnetic field, although the explanation is beyond the scope of this article (*1–3*) . The magnetic field encircling the source current of a tangentially oriented dipole has a component perpendicular to the sphere surface and therefore can be measured by a gradiometer oriented perpendicular to the surface. Because a head differs in shape from a sphere and contains boundaries between regions of differing electrical conductivity, radially oriented dipoles and volume currents may contribute to the magnetic field perpendicular to the head surface. By comparison, electroencephalography (EEG) measures primarily volume currents associated with both radially and tangentially oriented dipoles.

EEG is still the mainstay of noninvasive recording of brain electrical activity, but MEG is considered to be potentially more effective in the three-dimensional localization of focal neuron events. MEG may be superior to EEG in spatial localization of current sources because the scalp and skull are transparent to the associated magnetic fields, whereas they smear and distort the volume currents measured by the EEG. In addition, because MEG measures primarily the tangential component of intracranial sources, computing for source localization by means of a model is simpler than for EEG, which measures the combination of radial and tangential sources and is also dependent on the conductivities of the various cerebral tissues (*4*). These possible advantages of MEG have encouraged research of magnetic fields associated with many brain activities (*5*). The location of intracranial current sources has been predicted by MEG, but confirmation of the findings requires direct recording from the brain (*6*). The challenge to MEG research is to show that the predictions are accurate. The study and treatment of epilepsy are ideal for addressing this challenge. The magnitude of the electrical and magnetic signals associated with epilepsy is large, and direct recording from the brain during surgical intervention in many patients with epilepsy can be used to verify the MEG findings.

The MEG recording of epileptiform activities was first described in 1977 (*7*). Recently, persons with epilepsy whose seizures originate in just one area of the brain and who are candidates for the surgical removal of this epileptogenic region have been the subjects of intensive MEG research studies (*8–20*). The noninvasive diagnostic procedures, namely EEG, computed tomography (CT), magnetic resonance imaging (MRI), and positron emission tomography (PET) often yield inadequate information for accurately determining the location of the epileptogenic focus within the brain. The

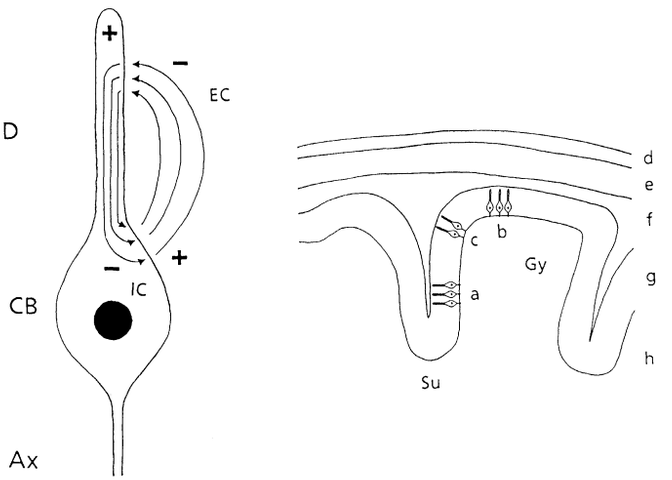

Fig. 1. (**Left**) Idealized cortical neuron. Fluctuations in membrane potential at the dendrite (D) induce compensatory intracellular (IC) and extracellular (EC) current flow; CB, cell body and nucleus, Ax, axon. (**Right**) Idealized cross section of scalp, skull, and brain. Cortical neurons oriented parallel to the scalp surface (a) produce tangential dipoles which can be measured by MEG. Those oriented perpendicular to the scalp surface (b) produce dipoles oriented radially and do not contribute to the component of the extracranial magnetic field perpendicular to the scalp. Neurons with intermediate orientation (c) produce dipoles with both tangential and radial components. Other features: d, scalp; e, skull; f, cerebrospinal fluid; g, cortex; h, noncortical brain or white matter; Su, sulcus; and Gy, gyrus.

invasive diagnostic techniques involve surgical intervention for recording directly from the surface of the brain with electrocorticography and subdural electrodes or from wire electrodes, called depth electrodes, inserted into the brain. These procedures have risks, and are costly and time consuming. If the epileptogenic region can be surgically removed, however, the patient may become completely free from seizures (*6*). MEG may decrease the need for surgical diagnostic procedures in patients with epilepsy by providing preoperative, noninvasive localization of the epileptogenic focus in three dimensions. It is estimated that approximately 50,000 persons in the United States are candidates for epilepsy surgery.

Epilepsy is characterized by recurrent abnormal synchronous discharges of large numbers of neurons within the brain. These discharges are seen in the EEG as brief high-amplitude electrical potential changes known as spikes or sharp waves (Fig. 3). Spikes have a duration of less than 70 msec, and sharp waves have a duration of 70 to 250 msec. When these discharges occur during seizures, they are called ictal discharges. Spikes and sharp waves are termed interictal discharges when they occur between seizures. Interictal discharges are recorded in the EEG more frequently than ictal discharges and therefore are somewhat easier to study. The anatomic origin of interictal discharges suggested by EEG is often close to the anatomic origin of ictal discharges found with subdural or depth electrodes, although this is not always the case. In the preoperative evaluation of a patient with epilepsy, it is important to determine the anatomic location of the onset of ictal discharges associated with clinical seizures, as these are the events causing the patient's disability. MEG may be able to provide additional information regarding these anatomic locations.

Instrumentation

The magnetic fields associated with the epileptiform events are approximately 1 picotesla (pT) and are measured with a superconducting detection coil coupled to a SQUID. Early instruments were single-channel detectors, but now instruments with four, five, or

seven channels spaced 2 to 3 cm apart are used. SQUID instrumentation has been well described (*1, 21, 22*). This article discusses only those aspects of the SQUID directly relevant to MEG.

The magnetometer has three components: detection and input coils, SQUID and electronics, and a cryogenic vessel (Dewar). The detection coils and the cryogenic vessel can be designed for MEG application, and the design will determine the spatial resolution and the ease of positioning the instrument over the patient's head (Fig. 2).

The detection coil is connected to the SQUID's input coil, and together they form a superconducting circuit that acts as a flux transformer. When a magnetic field is present at the detection coil, current flows in the superconducting circuit proportional to the instantaneous value of the magnetic flux present at the detection coil. The current flowing through the input coil impresses a field on the SQUID. A sensitive preamplifier and electronic circuit measure the response of the SQUID to this field; thus, the SQUID sensor and electronics can be regarded as a highly sensitive current to voltage converter, in excess of 10^7 V/A, whose output is linearly related to the instantaneous value of the magnetic flux passing through the detection coil. Two basic types of electronic circuitry drive the SQUID sensor, the so-called radio frequency (rf) and dc bias modes. Early versions of SQUID sensors incorporated rf electronics, but with improved technology dc SQUIDs are now two to three times more sensitive than the rf SQUID and are available in commercial instruments. Typical characteristics of commercially available SQUIDs are sensitivity better than 20 fT/Hz$^{1/2}$, linearity in excess of one part in 10^7, bandwidths extending from dc to hundreds of kilohertz, and slew rates of 10^5 to 10^6 ϕ_0/sec (*23, 24*).

In a magnetically unshielded setting, the detection coils are usually wound to form a gradiometer composed of a pickup coil placed close to the head and a similar compensating coil wound in the opposite direction placed parallel and a finite distance away (*1, 21*). Consequently, a spatially uniform magnetic field arising from a distant magnetic source, such as an elevator, produces equal and opposite signals in the two coils, and no induced current flows through the superconducting flux transformer circuit to the input coil of the SQUID. Sources close to the pickup coil, neuronal discharges with magnetic fields falling off as the square of the distance from the source, for example, induce unequal currents in the coils of the detector that do not cancel each other. Thus, an induced current flows through the input coil to the SQUID sensor and is detected as a voltage proportional to the rate of decay of the magnetic field along the axis of the gradiometer. Higher order gradiometers, either second or third order, are used to provide more stringent cancellation of distant fields in the electromagnetically noisy hospital setting. The penalty paid for this cancellation is that the total inductance of the detection coil (pickup and compensating) can no longer be matched to the inductance of the input coil of the SQUID at which maximum flux transport occurs, with consequent loss in sensitivity.

The choice of the detection coil diameter and the separation of the pickup and compensating coils, known as the baseline, determine the spatial resolution of the device. The effect of these factors on the measured field from a current dipole has been described in both homogeneous half-space and sphere models (*25*). Increased coil diameter averages the field across the area of the coil and leads to increased separation between the two recorded magnetic extrema, consequently overestimating the depth of the source. A knowledge of the diameter allows correction to be made for this parameter, but loss of spatial resolution is still present as a result of the broadening of the magnetic field distribution, which interferes with accurate determination of the extrema positions. For discussion of the detection coil, correction curves for coil diameters, and analysis of second-order gradiometers see (*25–27*). In MEG applications, typical coil dimensions are a coil diameter of 1.5 cm, a baseline of 4 cm, and an intercoil spacing in multichannel instruments of 2 cm.

Although the SQUID is sensitive enough to detect spontaneous magnetic fields of the brain and the gradiometer cancels distant magnetic fields, local background magnetic noise within the hospital setting (typically 1000 pT/Hz$^{1/2}$) remains a problem. The signal-to-noise ratio (ranging from 3:1 to 10:1) of the magnetic spikes and sharp waves obtained from patients in some laboratory sites is sufficiently good that the events can be seen in the unprocessed chart recording (*20*). Nonetheless, background magnetic noise contributes significantly to apparent variability and uncertainty in the signal and makes localization of the source less certain (*6*). Averaging of about 10 to 20 events to improve the signal-to-noise ratio has been performed at some laboratories with some success, although at the risk of also averaging variations in events (*8, 18*).

Initial attempts at noise cancellation used three additional orthogonally oriented magnetometers within the dewar that were located farther from the patient's head than the signal detector (*28*). These SQUIDs measured environmental noise, which was then electronically subtracted from the recording signal. Environmental noise subtraction was previously obtained by placing the instrument in a constant magnetic field. This procedure was successful for noise below 10 Hz, but was unsuccessful for the frequencies of interest in epilepsy above 10 Hz, probably because of the variable nature of noise sources at higher frequencies.

Despite the noise reduction achieved with the gradiometer and the noise reduction channels and electronics, further shielding is necessary for clinical MEG studies. This further shielding can be supplied only by a magnetically shielded room, which can offer a millionfold reduction in the environmental noise. This chamber employs a combination of high permeability material for magnetic

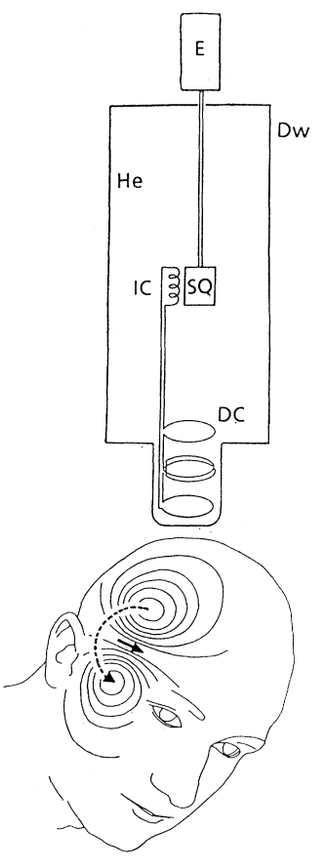

Fig. 2. Schematic of a SQUID gradiometer and the magnetic field of an idealized intracranial current source. The gradiometer is maintained perpendicular to the head surface during the recording sessions. The component of the magnetic flux perpendicular to the head, passing through the loops of the detection coil (DC), induces a current that is transferred by the input coil (IC) to the SQUID (SQ). The SQUID electronics (E) then convert the signal to a voltage proportional to the magnetic flux at the detection coil. Liquid helium (He) maintains the inside of the Dewar (Dw) at superconducting temperatures. The solid arrow represents an idealized intracranial current source oriented tangentially to the scalp surface. The dotted arrow represents the magnetic flux that encircles the current dipole and is oriented at a right angle to the direction of the current dipole. The concentric lines represent isoflux contours on the head surface (magnetic field map).

shielding and aluminum for eddy current shielding (*29–31*). Reduction of noise to a range from 3 $fT/Hz^{1/2}$ to 5 Hz has been reported. A more conservative approach financially and in construction terms is a room solely relying on eddy-current shielding having noise reduction levels to 100 $fT/Hz^{1/2}$ (*32*).

Cryogenic vessel design (*33*) is beyond the scope of this article, but the constraints imposed by a liquid helium system do have an impact on the recordings that are possible with MEG. In particular, the vessel cannot be tipped beyond 45° and a Dewar probe tip diameter of approximately 15 cm below a Dewar body of 35 cm in diameter imposes limitations on access to the head. Current technology limits to seven the number of sensors that can be accommodated within a cryogenic vessel.

The number of sensors available limits the area of the head measurable at any one time. This area is small relative to the large area that must be scanned to make a magnetic field map, and the independent recordings at each of these sites must be integrated over the complete head. Careful attention must be paid to integrating only those recordings associated with similar events.

Data Collection

The effectiveness of the MEG data collection and analysis methods is dependent on the nature of the signals and the source that generates these signals. The signals of interest in epilepsy research are ictal and interictal electrical discharges from an epileptogenic brain region. These discharges are detectable on the scalp because of volume currents, that is, extracellular currents throughout the head that complete the circuit of the intracellular current flow. The EEG is recorded with electrodes applied to the scalp surface and measures the potential difference between electrode pairs that arises from the volume current flow across the resistive scalp. Interictal spikes and sharp waves occur intermittently on the EEG as brief high-amplitude discharges within lower amplitude background activity. Ictal events, or seizures, which occur less frequently, have a variable appearance on the EEG (*34*). The EEG is usually recorded simultaneously at many locations over the head, and the region of maximum electrical potential during a spike or sharp wave can easily be determined. The scalp locations of the maximum potentials in a patient may be very similar for consecutive spikes and sharp waves, may vary several centimeters from one epileptiform event to the next, or may be so far apart as to suggest independent sources for the discharges (*20*). The MEG record closely resembles that of the EEG, although the signal-to-noise ratio is presently better for the EEG.

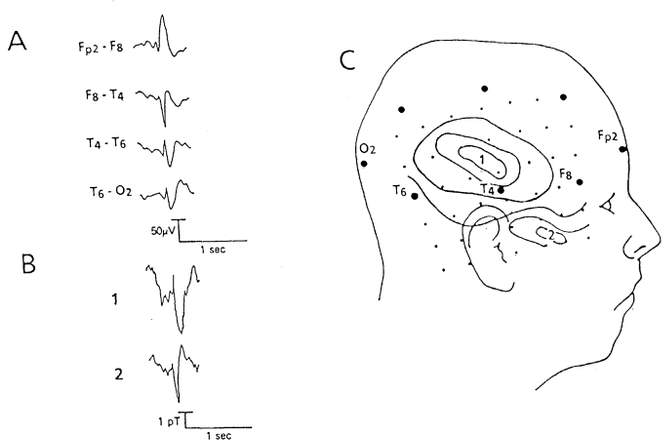

Fig. 3. (**A**) The EEG recording of an epileptiform spike. The four simultaneous signals, recorded from a patient's scalp, represent the difference in electrical surface potential between pairs of adjacent electrodes located over the front (F_{p2} and F_8), side (T_4 and T_6), and back of the head (O_2). (**B**) Recording of magnetic signals. These two magnetic spikes were recorded at different times but each was recorded simultaneously with an EEG spike that was visually similar to the EEG spike shown above. (**C**) The magnetic field map. The map was constructed from the peak-to-peak amplitudes of magnetic spikes that were recorded sequentially at 42 locations (small dots) over the side of the head and that were associated with similar EEG spikes. The solid lines represent magnetic isoflux lines. The first magnetic spike (from B) was recorded with the magnetometer positioned at a magnetic maximum (1) and the second spike at a magnetic minimum (2). The large dots represent EEG electrode locations.

The variability in the EEG signals is the result of the fact that epileptogenic regions are not pinpoints. An area that produces a spike or sharp wave on the EEG involves at least 6 cm^2 of cortical brain tissue (*35*) and probably represents the size that can be detected with present magnetometers. When the electrical activity of such a region is measured with electrocorticography, the whole area may discharge synchronously or shifting subregions may discharge independently (*36*). Some patients may have more than one epileptogenic region that, although located on the same side of the brain, are clearly distinct anatomically and discharge asynchronously.

The area covered by single detectors, and even by arrays of seven detectors, is small relative to the area that must be scanned to describe adequately the magnetic field for localization of the source. Because the magnetometer must be moved to record sequentially at many locations over the head and because of the intermittent nature of epileptiform events, recording sessions may last several hours, with complete mapping of the magnetic field distribution across the surface of the head requiring several days. Continuous recording, for example, of 7 channels of MEG and 14 channels of EEG produces large amounts of data. Eventually, the intermittent epileptiform discharges must be extracted from the continuous background activity. Various methods of accomplishing this extraction have been devised, with each method finally resulting in brief "windows" of data that include the epileptiform event and a few seconds of background activity preceding and following the event (*8, 12–15, 20*). These windows of digitized 12-bit data usually have been filtered at a bandwidth of 1 to 35 or 50 Hz, and sampled at rates of 128 to 256 samples per second. Both ictal (*19*) and interictal discharges (*8–18, 20*) and certain events that are not clearly epileptiform, but are focal and rhythmic, have been mapped in epileptic patients (*12, 18, 37*).

For MEG recording, a thin, closely fitting nylon or plastic cap is placed on the patient's head after application of the EEG electrodes, and a grid of planned recording points is marked on the cap (usually 2 to 4 cm apart). The magnetometer is then moved sequentially to each recording point with the detection coil placed parallel to the head surface (gradiometer axis perpendicular to the head surface). The EEG is recorded simultaneously so that the MEG may be compared with an established technique that provides immediate identification of epileptiform discharges and artifacts. This feature is particularly important when the magnetometer is placed at a recording point where the magnetic field is expected to be small or zero during an epileptiform discharge. The EEG then provides the only information that an epileptiform event has in fact occurred. An additional reason for the simultaneous recording of the MEG and EEG is the possibility of comparing MEG and EEG maps to obtain both the tangential and radial components of the dipole source.

Data Analysis

The magnetic field expected from a current source can be calculated from electromagnetic theory if certain conditions are met. The first is that the source is reasonably small and can be modeled as

a current dipole in a conducting sphere or infinite half space. For a gradiometer that is perpendicular to the surface of the sphere during recording, the detectable magnetic field is only associated with the component of the current source that is tangential to the sphere. Two magnetic maxima, or extrema, of opposite sign are predicted to be found on the surface orthogonal to the EEG dipolar potential distribution (*4*) (Fig. 2). Clinically, the two magnetic maxima are detected consistently even though the epileptogenic region is not a pinpoint source and the head is neither a perfect sphere nor an infinite half space (*8–20*). Once the magnetic field map with two extrema is obtained, a three-dimensional location for the source is calculated with one of several models discussed below.

One of the major difficulties in data analysis is the small area measured by the magnetometers relative to the large area that must be scanned to make a magnetic map. Present multichannel magnetometers only measure the magnetic field over an area of at most 5.5 cm in diameter (*6*), which is insufficient to characterize both of the magnetic extrema needed for mapping.

Production of the magnetic field map from sequential measurements presents difficulties. First, because of the changing nature of discharges arising in the epileptogenic region, consecutive spikes and sharp waves cannot be assumed to be identical. In addition, there is variability in the discharges because of variation in both background brain activity and environmental noise (*8, 13, 20*). Finally, uncertainty of the exact position of the detector at each location over the head may add to these difficulties. Several different techniques have evolved in an attempt to handle this variability. All rely on the simultaneously recorded EEG.

One technique is to examine carefully each of the EEG spikes or sharp waves recorded from a patient and to identify similarities and differences in their morphological characteristics and location of maximum electrical potential on the scalp. Interictal discharges that are visually similar in these two respects are grouped together, and then a representative discharge is chosen at each detector position. The magnitude of the magnetic signal (baseline-to-peak or peak-to-peak) associated with the representative discharge is measured and from these individual measurements a magnetic field map across detector positions is produced. The procedure is repeated for each distinctly different EEG spike or sharp wave pattern. The result is usually several EEG epileptiform patterns, each with an associated magnetic field map (*15, 20*).

The chief advantage of this technique is that the underlying variability inherent in the epileptogenic region is probably preserved. The technique may characterize the variability of the epileptogenic region, indicate the extent of the area, and suggest the possibility of separate and independent regions in a single patient. A disadvantage is that the recurrent EEG patterns in the spike and sharp wave and the location of maximum potential on the scalp must first be elucidated. The identification of patterns and the choice of the representative spikes at each recording position are by visual inspection and depend on the experience and judgment of the investigator, although it may be possible to establish quantifiable criteria and to automate the process. A good signal-to-noise ratio during each interictal discharge, important for all the data analysis methods, is particularly relevant for this technique (*20*).

A second technique is to take consecutive EEG epileptiform events (spikes and sharp waves) obtained at a single detector position, align the EEG signals by a chosen common marker (for example, the first peak in one of the EEG channels), and average the associated magnetic signals. Usually 10 to 20 interictal discharges are included in the average. The procedure is repeated at each of the detector positions, and from the averaged signals a magnetic field map is produced. Usually one or two components of the averaged interictal discharge are examined in this manner. The result is a magnetic field map for each component evaluated (*8, 13*).

The advantage of the second technique is that it processes all epileptiform events without prior interpretation. In addition, the method may eliminate spurious irregularities in the magnetic field map that are caused by variation in the background brain activity or environmental noise. A disadvantage is that discharges arising from spatially separated subregions within the epileptogenic regions will be averaged together, and this averaging yields a single three-dimensional point for events that may spread over several centimeters of cerebral cortex. This may not be a problem if the subregions are relatively close to one another and it is remembered that the three-dimensional point represents an average spatial location for a larger epileptogenic region. However, discharges arising from anatomically separate and physiologically independent epileptogenic regions may be averaged together to produce a three-dimensional location that represents neither of the epileptogenic regions. Also, events that occur independently of one another and have differently oriented magnetic fields may be averaged and appear to be related in time, although if the two events can be seen in the epileptiform discharges prior to averaging, this problem may be addressed.

A third technique examines windows of EEGs by means of the fast Fourier transform (FFT) for frequency peaks. The EEG and simultaneous MEG are filtered at a 2-Hz bandwidth around a peak of interest, and the covariance between the MEG and one of the EEG channels is calculated. The result is divided by the variance of the specified EEG channel to compensate for variability in intensity of the discharge arising from the epileptogenic region and is termed the relative covariance (RC). In-phase and out-of-phase MEG and EEG signals should yield positive or negative RC values, respectively. The procedure is repeated for segments of simultaneous EEG and MEG at each detector position, and these RC values are then plotted on the recording grid to produce a map with contour lines that represent constant values of RC. If the discharges arising in the epileptogenic region have been similar throughout the recording and have had a similar representation on the EEG, the overall spatial distribution of the RC values should reflect that of the magnetic field. The RC map is examined for the presence of two oppositely signed and maximal regions of RC values, which are assumed to reflect the two extrema of the magnetic field. For a given set of segments of EEG and MEG, this procedure may be repeated at different bandwidths of interest and use different EEG channels to determine RC, yielding several RC contour maps for the data set (*12, 14, 18, 37*).

The FFT technique permits examination of the magnetic field associated with selected frequency bands within interictal discharges, an analysis that is not available from the first two techniques. In addition, it permits evaluation of abnormal rhythmic activities that may not be as sharply defined in the EEG as spikes and sharp waves but nonetheless may be important in the study of epilepsy, such as focal slow waves. The major disadvantage is inability to follow the time evolution of the event. In addition, when abnormal activity occurs in the EEG window, there is some difficulty ascertaining that the chosen FFT peak actually represents the abnormal EEG activity. Spikes and sharp waves have several components in the frequency domain that may make analysis more difficult. The maps represent RC values and not magnetic field strength; therefore an additional method must be devised to estimate the magnitude of the source. If more than one interictal discharge occurs during a specified window, the evaluation of the events, in a sense, averaged. This technique would then have additional strengths and disadvantages similar to the averaging technique mentioned above.

Although different research laboratories have promoted one or another technique, use of one technique does not preclude use of

another, and in practice each laboratory uses a combination of techniques to handle the variability in the signal. Each of the techniques relies on the EEG in one way or another to produce the magnetic field map from data sequentially obtained at different detector positions. The underlying assumption is that the recorded EEG and MEG signals are tightly coupled. However, the EEG may be preferentially sensitive to radially oriented sources such as occur in gyri at the outer surface of the brain, and the MEG may be preferential to tangentially oriented sources occurring in the infoldings, or sulci, of the brain. Since these regions are anatomically separate, one would expect the signals seen in the EEG and MEG to be loosely coupled to one another (*6, 38*).

The difficulties in data analysis that are incurred because of the need to construct the magnetic field map from sequential measurements will diminish when it is possible to map the total magnetic field of single events with a multichannel detector. Enough channels are required to obtain both magnetic extrema simultaneously and with good signal-to-noise ratio (*6, 18, 37*). The MEG could then be interpreted independently of the EEG. The above data analysis technique could still be useful but would be applied separately to the MEG and EEG for comparison of the results.

Models of Magnetic Field Sources

The initial data analysis in MEG produces a magnetic field map with two oppositely signed magnetic maxima. However, this alone does not give the three-dimensional location of the event. Various models of the source and the head must be utilized to predict the source location based on the magnetic field map. The determination of this location from the clinically measured magnetic field is termed the "inverse problem," for which there is no unique solution. Nonetheless, by using fairly simple models for the source and the head (described below), a parsimonious prediction of the source location can be made. More complicated models of the source and head are best evaluated with a "forward solution," where a mathematically described source is placed in a complex model of the head and the magnetic field expected at the surface of the head model is calculated based on Biot and Savart's law [see, for example, (*4*)]. This calculated field is compared to the clinically measured magnetic field. The model source is then iteratively moved within the head model until a best fit is obtained between the calculated field and the clinically measured field map.

Several models for the source have been proposed, the simplest being the single current dipole (*2*). Several studies have shown that for isolated and multiple independent sources, and for multiple sources arranged in a planar sheet, this model is a reasonable approximation (*3, 39*).

Two relatively simple methods of the head and several more complicated models have been proposed. One of the simple models is the infinite half space, which has been proposed for sources situated close to the head surface. In this model, the source lies below the head surface midway between the two magnetic extrema and at a depth determined by the separation of the maxima divided by 2 (*1*). The magnetic extrema recorded in epileptic patients who are surgical candidates often occur over the side of the head, a surface that is relatively flat. However, this model has obvious limitations because the head is not an infinite half space.

The second simple model is the sphere (*40*), which approximates the topology of the top and back, but not the side, of the head. In this model, the predicted location of the source again lies below the head surface midway between the two magnetic extrema (*21*). The depth below the surface is determined by the angle subtended at the center of the head by the two extrema. The center of the head is usually determined from the best-fit sphere to the x-ray skull films, computed tomography, or magnetic resonance imaging scans. However, for magnetic maxima occurring over the side of the head, several researchers have found that different choices of placement of the center of the model sphere greatly affect the predicted three-dimensional location of the source (*37, 41, 42*).

A study of a current dipole placed in the cranium of a human cadaver (intracranial space replaced by conducting gel) showed that the surface topology of the side of the head distorted the magnetic extremum occurring over the cheekbone and attributed this finding to the nonspherical head surface, the changing distance of the detector from the center of the head, and the changing orientation of the detector relative to a model sphere (*41*). A clinical study of epileptic patients examined the relation of head topology to the clinically measured magnetic fields maps; control studies were conducted to account for the position and orientation of the detector relative to the patient's head, and the researchers assumed that there was no contribution from volume currents to the measured magnetic field. The results suggested that although head topology distorted the extrema, certain recurrent features of the clinical maps, namely, lower than expected magnitude of the extrema located over the cheekbone, and a null point in the magnetic field that was not halfway between the two extrema, were not accounted for and that possible contribution from volume currents should be evaluated (*43*).

Several models have recently been proposed that more realistically represent the shape of the intracranial compartment, skull, and surface topology of the scalp. Employing numerical methods, these models include both the intracellular and volume current contributions to the measured magnetic field. A representation of the brain by a homogeneous body has produced encouraging results compared with a sphere, especially in the frontotemporal region (*44*). A problem to be overcome for on-line analysis of the neuromagnetic data is the lengthy computational time required for the algorithm. An alternative approach includes simultaneous analysis of both the EEG and MEG field distributions (*45, 46*). A drawback of this technique is the influence of the volume conductor on the EEG, which requires accurate knowledge of the conductivities and shape of the brain tissue, cerebrospinal fluid, skull, and scalp.

Validation

Any noninvasive technique that predicts the three-dimensional source of brain events must be tested for the accuracy and precision of its prediction. Epileptiform discharges arise from an epileptogenic region of the brain and not a "point" source (*47*). When patients with seizures are considered for surgical treatment, the accuracy and precision of localization of sources by MEG become crucial issues. Other noninvasive diagnostic procedures (scalp-recorded EEG, MRI, CT, and PET) are not good measures for validating the localizing ability of MEG (*6*). MEG predictions must be validated by direct recording from the brain by electrocorticography (ECoG), subdural electrodes, or depth electrodes. ECoG is used during epilepsy surgery to delineate the extent of the epileptogenic region and the method usually shows several independently discharging subregions within the overall epileptogenic region (*48*). These epileptiform discharges differ from those of the scalp-recorded EEG in number, amplitude, and morphology (*49*). Similar differences may occur between MEG and ECoG. Thus, MEG findings should be validated by comparing the MEG-predicted epileptogenic region with the region found by direct recording from the brain (*16, 20*). There appears to be good correlation between epileptogenic regions predicted by MEG and those found by ECoG, although techniques

to evaluate the accuracy and precision of the predictions are still being explored (*18–20*). Additional validation and testing may be possible by simultaneous recording of the MEG and brain electrical activity from subdural or depth electrodes.

Future Directions

The efficient study of epilepsy by MEG depends on the ability to rapidly and completely record the magnetic fields of ictal and interictal discharges in a magnetically quiet environment. This will require a recording site within a shielded room and an instrument with enough detectors to measure both magnetic extrema at the same time. When both of these criteria are met, it will be possible to study the changing magnetic field patterns and predicted current source location of a single interictal discharge. These studies may provide insight into whether superficial interictal discharges recorded in the lateral temporal lobe arise locally or are precipitated by discharges from deeper structures in the medial temporal lobe. Although magnetic fields and source locations of seizures have been studied with single-channel magnetometers, the recording of 30 to 40 seizures in each patient to complete a magnetic field map is time-consuming and requires patients who have frequent stereotyped seizures (*19*). Future instrumentation should permit prediction of current source locations during the onset and propagation of seizures in a greater number of patients. MEG may then become a clinically important noninvasive procedure for the presurgical localization of the epileptogenic region. Comparison of localizations of ictal and interictal discharges may provide clearer insight into their relationship. Study of the propagation of seizures may provide important anatomic information about the paths of seizure spread and may validate MEG as a technique for studying patterns of communication among different neuronal populations within the brain.

REFERENCES AND NOTES

1. F. Grynszpan and D. B. Geselowitz, *Biophys. J.* **13**, 911 (1973).
2. D. Cohen and H. Hosaka, *J. Electrocardiol. (San Diego)* **9**, 409 (1976).
3. B. N. Cuffin and D. Cohen, *IEEE Trans. Biomed. Eng.* **24**, 372 (1977).
4. S. J. Williamson and L. Kaufman, *J. Magn. Magn. Mater.* **22**, 129 (1981).
5. S. Sato and P. D. Smith, *J. Clin. Neurophysiol.* **2**, 173 (1985).
6. S. Sato, D. F. Rose, C. V. Kufta, W. H. Theodore, in *Proceedings of the Workshop on Biomagnetism*, Turin, Italy, 1 to 6 September 1986.
7. J. R. Hughes, J. Cohen, C. I. Mayman, M. L. School, D. E. Hendrix, *J. Neurol.* **217**, 79 (1977).
8. D. S. Barth, W. Sutherling, J. Engel, Jr., J. Beatty, *Science* **218**, 891 (1982).
9. I. Modena *et al.*, *Electroencephalogr. Clin. Neurophysiol.* **54**, 622 (1982).
10. S. Barbanera, G. B. Ricci, I. Modena, *Nuovo Cimento* **2**, 547 (1983).
11. G. B. Ricci, *ibid.*, p. 517.
12. R. M. Chapman, G. L. Romani, S. Barbanera, R. Leoni, *Lett. Nuovo Cimento* **38**, 549 (1983).
13. D. S. Barth, W. Sutherling, J. Engel, Jr., J. Beatty, *Science* **223**, 293 (1984).
14. G. B. Ricci *et al.*, in *Biomagnetism: Application and Theory*, W. Weinberg, G. Stroink, T. Katila, Eds. (Pergamon, New York, 1985), pp. 304–310.
15. S. Sato, D. Rose, R. Porter, in *ibid.*, pp. 261–263.
16. S. Sato *et al.*, in *ibid.*, pp. 311–315.
17. W. Sutherling, D. S. Barth, J. Beatty, in *ibid.*, pp. 249–260.
18. G. B. Ricci *et al.*, *Electroencephalogr. Clin. Neurophysiol.* **66**, 358 (1987).
19. D. Rose, S. Sato, C. Kufta, *Neurology (Suppl.)* **36**, 83 (1986); W. W. Sutherling *et al.*, *Ann. Neurol.* **21**, 548 (1987).
20. D. F. Rose *et al.*, *Ann. Neurol.* **22**, 348 (1987).
21. G. L. Romani, S. J. Williamson, L. Kaufman, *Rev. Sci. Instrum.* **53**, 1815 (1982).
22. J. B. Gallop and B. W. Petley, *J. Phys. E.* **9**, 417 (1976); R. E. Sarwinski, *Cryogenics* **17**, 671 (1977); J. Clarke, in *Superconducting Applications: SQUIDs and Machines*, B. B. Schwartz and S. Foner, Eds. (Plenum, New York, 1977), p. 67; S. J. Swithenby, *J. Phys. E.* **13**, 801 (1980).
23. R. L. Fagaly, *Sci. Prog. (London)* **71**, 181 (1987).
24. ϕ_0 is the flux quantum (2.07×10^{-15} Weber) in multiples of which the magnetic field is quantized in the superconducting loop that forms the SQUID sensor.
25. S. J. Williamson and L. Kaufman, *Biomagnetism*, S. N. Erne, H.-D. Hahlbohm, H. Lubbig, Eds. (de Gruyter, Berlin, 1981), pp. 353–402.
26. G. M. Baule and R. J. McFee, *J. Appl. Phys.* **36**, 2066 (1965).
27. J. E. Opfer, Y. K. Yeo, J. M. Pierce, L. H. Rorden, *IEEE Trans. Magn.* **MAG-9**, 536 (1974).
28. Neuromagnetometer System, model 607 (operator and service manual), Biomagnetic Technologies, Inc., San Diego, CA.
29. D. Cohen, *Rev. Phys. Appl.* **5**, 53 (1970).
30. V. O. Kelha *et al.*, *IEEE Trans. Magn.* **MAG-18**, 260 (1982).
31. A. Mager, in (*25*), pp. 51–78.
32. J. E. Zimmerman, *J. Appl. Phys.* **48**, 702 (1977).
33. ———, in *Biomagnetism—An Interdisciplinary Approach*, S. J. Williamson, G. L. Romani, L. Kaufman, I. Modena, Eds. (Plenum, New York, 1983), pp. 43–67.
34. S. Sato and D. F. Rose, in *Neurologic Clinics*, R. J. Porter and W. H. Theodore, Eds. (Saunders, Philadelphia, 1986), vol. 4, no. 3, pp. 509–529.
35. R. Cooper, A. L. Winter, H. J. Crow, W. G. Walter, *Electroencephalogr. Clin. Neurophysiol.* **18**, 217 (1965).
36. H. Jasper, B. Pertuisset, H. Flanigin, *Arch. Neurol. Psychiatry* **65**, 272 (1951).
37. G. L. Romani and R. Leoni, in (*14*), pp. 205–220.
38. D. Cohen and B. N. Cuffin, *Electroencephalogr. Clin. Neurophysiol.* **56**, 38 (1983).
39. Y. Okada, in (*14*), pp. 266–272.
40. Calculations have been made for the external magnetic field of a current dipole inside a sphere [F. Grynszpan, thesis, University of Pennsylvania (1971)], oblate and prolate spheroids (*3*), and for an array of aligned and random dipoles [B. N. Cuffin and D. Cohen, *J. Appl. Phys.* **48**, 3971 (1977)].
41. D. S. Barth, W. Sutherling, J. Broffman, J. Beatty, *Electroencephalogr. Clin. Neurophysiol.* **63**, 260 (1986).
42. F. Pistella, *Phys. Med. Biol.* **32**, 115 (1987).
43. D. F. Rose, S. Sato, P. D. Smith, J. White, *ibid.*, p. 59.
44. M. S. Hamalainen and J. Sarvas, *ibid.*, p. 91.
45. D. Cohen and B. N. Cuffin, *ibid.*, p. 85.
46. C. J. Stok, J. W. H. Meijs, M. J. Peters, *ibid.*, p. 99.
47. P. Gloor, in *Surgical Treatment of the Epilepsies*, J. Engel, Jr., Ed. (Raven, New York, 1987), pp. 97–100.
48. C. Ajmone-Marsan, in *Electrodiagnosis in Clinical Neurology*, M. J. Aminoff, Ed. (Churchill Livingstone, New York, 1980), pp. 167–196.
49. K. Abraham and C. Ajmone-Marsan, *Electroencephalogr. Clin. Neurophysiol.* **10**, 447 (1958).

50. We thank B. J. Hessie for critical review of the manuscript.